HMG Advance Access published April 19, 2011

Human Molecular Genetics, 2011 **1–13**
doi:10.1093/hmg/ddr123

Copy number variations on chromosome 12q14 in patients with normal tension glaucoma

John H. Fingert[1,*], Alan L. Robin[4,5,6], Jennifer L. Stone[4], Ben R. Roos[1], Lea K. Davis[2], Todd E. Scheetz[1], Steve R. Bennett[7], Thomas H. Wassink[2], Young H. Kwon[1], Wallace L.M. Alward[1], Robert F. Mullins[1], Val C. Sheffield[3,8] and Edwin M. Stone[1,8]

[1]Department of Ophthalmology and Visual Sciences, [2]Department of Psychiatry and [3]Department of Pediatrics, Carver College of Medicine, University of Iowa, Iowa City, IA, USA and [4]Glaucoma Specialists, Baltimore, MD, USA, [5]Department of Ophthalmology and International Health, School of Medicine and [6]Bloomberg School of Public Health, Johns Hopkins University, Baltimore, MD, USA, [7]Department of Ophthalmology, University of Minnesota, Minneapolis, MN, USA and [8]Howard Hughes Medical Institute, Iowa City, IA, USA

Received October 4, 2010; Revised March 17, 2011; Accepted March 23, 2011

We report identification of a novel genetic locus (*GLC1P*) for normal tension glaucoma (NTG) on chromosome 12q14 using linkage studies of an African-American pedigree (maximum non-parametric linkage score = 19.7, max LOD score = 2.7). Subsequent comparative genomic hybridization and quantitative polymerase chain reaction (PCR) experiments identified a 780 kbp duplication within the *GLC1P* locus that is co-inherited with NTG in the pedigree. Real-time PCR studies showed that the genes within this duplication [*TBK1* (TANK-binding kinase 1), *XPOT*, *RASSF3* and *GNS*] are all expressed in the human retina. Cohorts of 478 glaucoma patients (including 152 NTG patients), 100 normal control subjects and 400 age-related macular degeneration patients were subsequently tested for copy number variation in *GLC1P*. Overlapping duplications were detected in 2 (1.3%) of the 152 NTG subjects, one of which had a strong family history of glaucoma. These duplications defined a 300 kbp critical region of *GLC1P* that spans two genes (*TBK1* and *XPOT*). Microarray expression experiments and northern blot analysis using RNA obtained from human skin fibroblast cells showed that duplication of chromosome 12q14 results in increased *TBK1* and *GNS* transcription. Finally, immunohistochemistry studies showed that TBK1 is expressed in the ganglion cells, nerve fiber layer and microvasculature of the human retina. Together, these data link the duplication of genes on chromosome 12q14 with familial NTG and suggest that an extra copy of the encompassed *TBK1* gene is likely responsible for these cases of glaucoma. However, animal studies will be necessary to rule out a role for the other duplicated or neighboring genes.

INTRODUCTION

Glaucomas are a group of common neurodegenerative diseases of the optic nerve and retinal ganglion cells. They are characterized by progressive cupping of the optic nerve head with resultant visual field loss. Elevated intraocular pressure (IOP) is a strong risk factor for glaucoma; however, glaucoma can occur at any IOP (1). Glaucoma is a common cause of visual disability and blindness (2,3). It has been estimated that, in 2010, over 60 million people worldwide will have glaucoma (4). The most common form of glaucoma in the USA is primary open-angle glaucoma (POAG) (5). POAG that occurs with IOP below an arbitrary threshold of 21 mmHg is often termed normal tension glaucoma (NTG).

Genes have a significant role in the pathogenesis of glaucoma. In the last two decades, 14 loci for Mendelian forms of open-angle glaucoma genes have been identified with genetic linkage mapping [*GLC1A* through *GLC1N* (6–9)], and glaucoma-causing genes have been discovered at two of these loci [myocilin (10) and optineurin (11)]. Mutations in the myocilin gene (*MYOC*, OMIM 601652) are associated with ~4% of cases of POAG that are usually characterized

*To whom correspondence should be addressed at: Department of Ophthalmology and Visual Sciences, Carver College of Medicine, University of Iowa, 1269B CBRB, 285 Newton Road, Iowa City, IA 52242, USA. Tel: +1 3193357508; Fax: +1 8774349041; Email: john-fingert@uiowa.edu

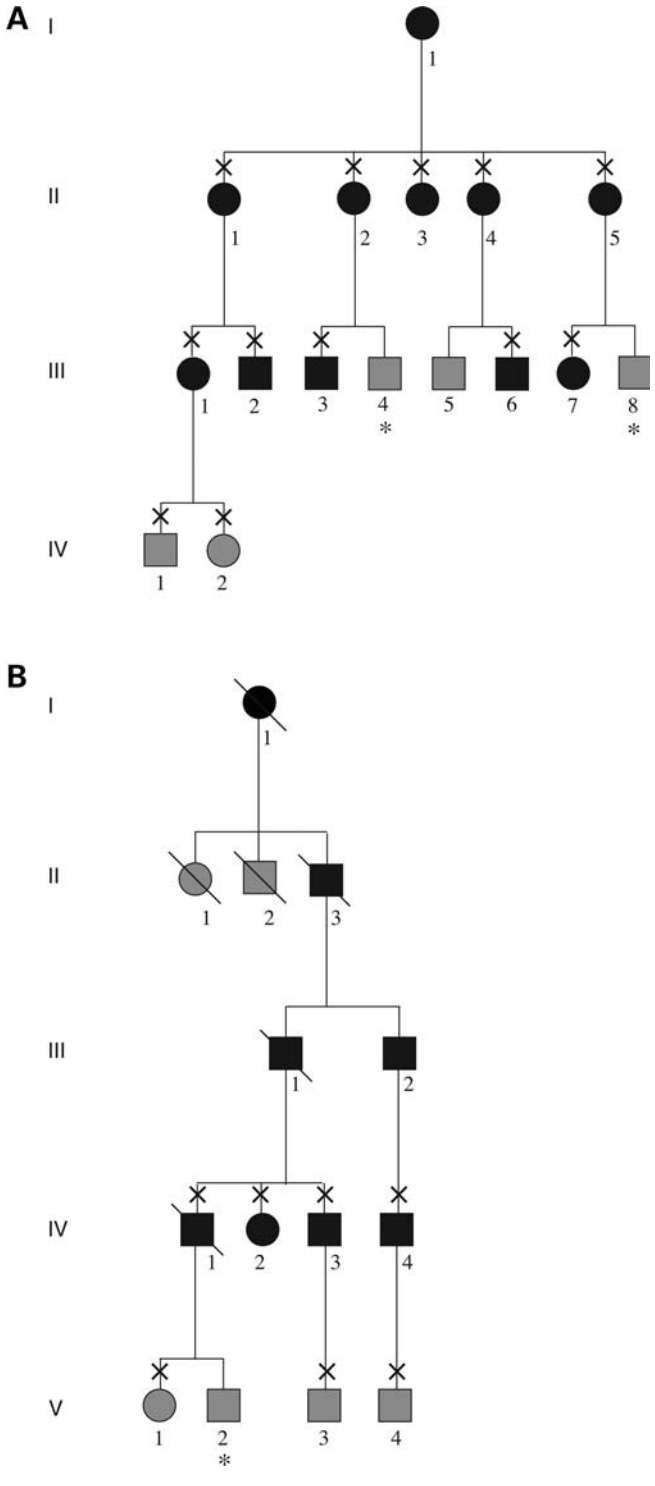

Figure 1. NTG pedigrees. Family members with NTG are indicated with black symbols, whereas those who did not meet diagnostic criteria for glaucoma but were considered to have unknown glaucoma status because of their age are indicated with gray symbols. Those family members with unknown glaucoma status because they were unavailable for examination are indicated with gray symbols and asterisks. (**A**) Pedigree 441. Members of this African-American pedigree with NTG who were included in the linkage studies are indicated with the symbol '×'. (**B**) Pedigree 458. Members of this Caucasian pedigree with NTG who contributed DNA samples are indicated with the symbol '×'. All affected family members in both pedigrees were found to carry their family's chromosome 12q14 duplication.

by markedly elevated IOP (12). The mechanism by which mutations in myocilin cause POAG was recently reviewed (13). Mutations in the optineurin gene (*OPTN*) have been associated with rare cases of NTG (11,14). The protein encoded by *OPTN* may have roles in exocytosis and apoptosis (15,16); however, the mechanism by which mutations in this gene cause glaucoma is unknown. A role for two additional genes, *WDR36* and *NTF4*, in glaucoma pathogenesis is controversial (17–24). Most glaucoma-causing mutations reported in myocilin and optineurin are missense, nonsense or frameshift mutations (12,16).

More recently, association studies have begun to identify genes that confer risk for POAG, which has a complex genetic basis. Thorleifsson *et al*. (25) mapped the first common genetic risk factor for POAG to a chromosome 7q31 locus that contains the caveolin-1 and caveolin-2 genes. Although the risk allele at this locus has not yet been discovered, preliminary data suggest that it may contribute as much as 12% population attributable risk for POAG. Similarly, risk alleles for NTG have also been identified in the *SRBD1* and *ELOVL5* genes via an association study (26).

Genes that cause congenital and developmental forms of glaucoma have also been identified. Coding sequence mutations in the *CYP1B1* gene have been associated with primary congenital glaucoma (27). Coding sequence mutations in the *PITX2* and *FOXC1* genes have similarly been associated with Axenfeld–Rieger syndrome, which may lead to a secondary form of glaucoma (28,29). Additionally, both duplications and deletions of *FOXC1* (30) and deletions of *PITX2* (31) have been linked to Axenfeld–Rieger syndrome, suggesting that copy number variation (CNV) may be an important mechanism in glaucoma pathogenesis.

Here we report mapping a novel NTG locus with a combination of pedigree-based and population-based studies. We also describe the first CNV associated with adult-onset open-angle glaucoma, which suggests a new mechanism of disease for NTG.

RESULTS

The authors performed complete ophthalmic examinations on 12 members of a large African-American pedigree with NTG (Pedigree 441, Fig. 1A). Ten of the 12 family members were diagnosed with POAG. The glaucoma in this pedigree is characterized by an early onset of disease (mean age at diagnosis = 36 years ± 8.2 years), thin central corneas (mean thickness = 509 ± 25 μm, right eye; 508 ± 31 μm, left eye) and low IOP (mean maximum IOP = 18.2 ± 4.1 mmHg, right eye; 16.7 ± 3.6 mmHg, left eye) as shown in Table 1. Five of the six affected family members with extensive ophthalmic records had a maximum IOP of ≤21 mmHg and met criteria for a diagnosis of NTG, whereas one family member had a maximum IOP of 22 mmHg.

Members of Pedigree 441 were first tested for disease-causing mutations in known glaucoma genes (myocilin and optineurin); however, no mutations were detected. Next, members of Pedigree 441 with NTG were studied by linkage analysis using genetic markers flanking the myocilin and

Table 1. Clinical features of patients with NTG in Pedigrees 441 and 458

Pedigree number	Pedigree symbol	Diagnosis	Age at diagnosis (years)	Max IOP, right eye (mmHg)	Max IOP, left eye (mmHg)	Corneal thickness, right eye (μm)	Corneal thickness, left eye (μm)	Cup-to-disc ratio, right eye (first examination)	Cup-to-disc ratio, left eye (first examination)	Visual field tests, right eye	Visual field tests, left eye	Glaucoma surgeries
Pedigree 441	II-1	NTG	46	20	17	NA	NA	1.00	1.00	Superior and inferior arcuate defects	Central defect with a temporal island	None
	II-3	POAG with borderline IOP	43	22	21	524	523	1.00	1.00	Superior and inferior arcuate defects splitting fixation	Superior altitudinal defect and inferior arcuate defect	Trabeculectomy, right eye; revised trabeculectomy, right eye
	II-4	NTG	38	20	16	NA	NA	0.99	0.99	Superior and inferior arcuate defects	Early superior arcuate defect	NA
	II-5	NTG	36	12	11	484	471	0.80	0.80	Non-specific changes	Nasal step	NA
	III-1	NTG	32	21	20	532	541	1.00	1.00	Superior and inferior arcuate defects and nasal steps	Superior and inferior arcuate defects and nasal steps	Argon laser trabeculoplasty, both eyes
	III-7	NTG	23	14	15	496	497	0.90	0.80	Decreased superior sensitivity	Decreased central and inferior sensitivity	None
	Average for glaucoma patients	—	36 ± 8.2	18.2 ± 4.1	16.7 ± 3.6	509 ± 25	508 ± 31	0.95 ± 0.083	0.93 ± 0.10	—	—	—
	IV-1	No glaucoma	NA	14	16	568	582	0.30	0.30	Full	Full	None
	IV-2	NTG suspect	NA	19	20	573	601	0.35	0.20	Full	Full	None

Continued

Table 1. *Continued*

Pedigree number	Pedigree symbol	Diagnosis	Age at diagnosis (years)	Max IOP, right eye (mmHg)	Max IOP, left eye (mmHg)	Corneal thickness, right eye (μm)	Corneal thickness, left eye (μm)	Cup-to-disc ratio, right eye (first examination)	Cup-to-disc ratio, left eye (first examination)	Visual field tests, right eye	Visual field tests, left eye	Glaucoma surgeries
Pedigree 458	III-1	POAG with borderline IOP	NA	21	22	NA	NA	NA	NA	Severely constricted with a central island of visual field	Severely constricted with a central island of visual field	Argon laser trabeculoplasty, left eye
	III-2	NTG	32	14	14	NA	NA	NA	NA	Constricted visual fields	Constricted visual fields	None
	IV-1	NTG	17	20	20	NA	NA	0.90	0.90	Severely constricted	Severely constricted	Argon laser trabeculoplasty, right eye
	IV-2	POAG	32	26	24	NA	NA	NA	NA	Temporal wedge and pericentral defects	Superior arcuate/ altitudinal defect	None
	IV-3	NTG	33	17	17	NA	NA	NA	NA	Extensive visual field loss	Extensive visual field loss	None
	IV-4	NTG	29	16	16	NA	NA	0.80	0.80	Marked visual field loss	Marked visual field loss	None
	Average for glaucoma patients	—	29 ± 6.7	19.0 ± 4.3	18.8 ± 3.8	NA	NA	0.85 ± 0.071	0.85 ± 0.071	—	—	—

Clinical data from Pedigree 458 was collected from a previously published report (35). Standard deviations are given for age at diagnosis, maximum IOP, corneal thickness and cup-to-disc ratios.

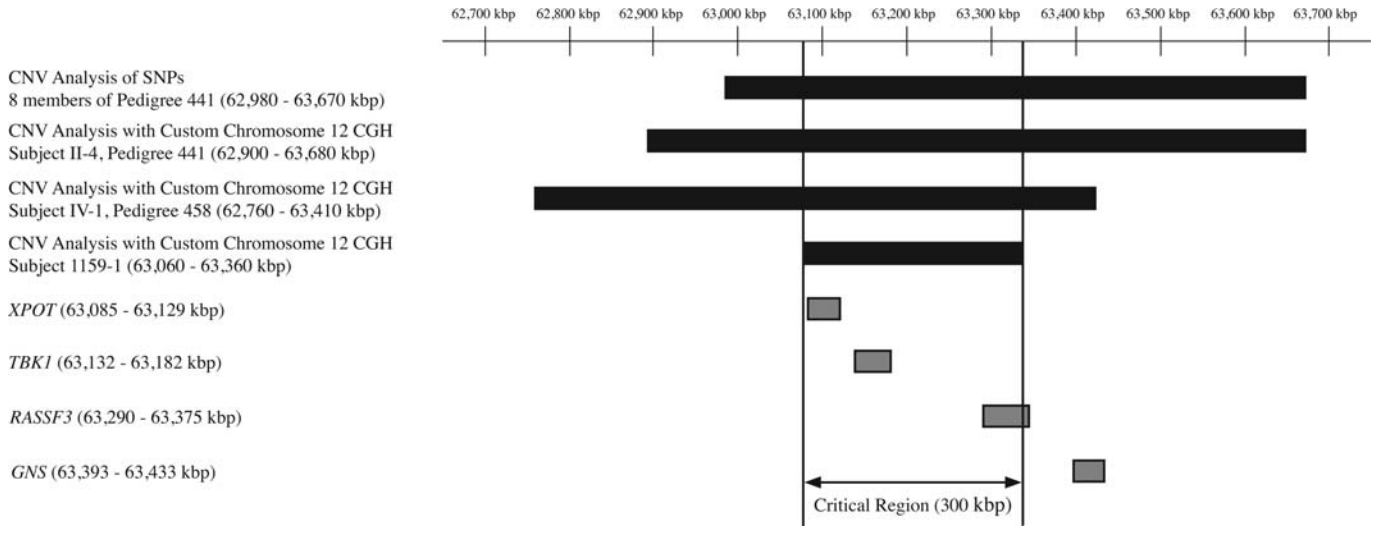

Figure 2. CNV analysis of NTG patients. Members of Pedigree 441 with NTG were investigated for CNVs by analyzing SNPs that were typed as part of the linkage analysis, by genome-wide CGH studies and by focused chromosome 12q14 CGH studies. The extent of the duplication detected in Pedigree 441 by these methods is represented by a black box. Similar analyses revealed overlapping but unique duplications in two unrelated NTG patients (Fig. 1B, Pedigree 458, IV-1 and Subject 1159-1). The extent of the duplications in these subjects is also represented by black boxes. The positions of known genes encompassed by these duplications are represented by gray boxes.

optineurin loci. Glaucoma in this pedigree was not linked to either of these loci. These initial studies ruled out a role for myocilin and optineurin in causing NTG in the pedigree and suggested the presence of a novel glaucoma-causing gene.

Pedigree 441 was next studied by genome-wide linkage analysis to map the gene that causes the family's glaucoma. The 10 family members with NTG were genotyped with 660 000 single-nucleotide polymorphisms (SNPs), using microarray technology. Analysis of the genotypes identified the largest cluster of linked SNPs on chromosome 12q14 which produced the genome-wide maximum non-parametric linkage (NPL) score of 19.7 and the genome-wide maximum LOD score of 2.7 ($\theta = 0$). No other loci with significant evidence for linkage were identified (the next highest NPL score was 6.0). All 10 affected family members share at least one allele of 1869 contiguous SNPs on chromosome 12q14 that defines a 9.47 Mbp locus that is bounded by the centromeric SNP *rs12227270* and the telomeric SNP *rs7488555*. The SNP-based linkage analysis was confirmed by genotyping the same 10 affected family members with nine short tandem repeat polymorphism (STRP) markers in the chromosome 12q14 locus. All nine STRP markers had maximum LOD scores at $\theta = 0$, and marker *D12S359* produced the maximum LOD score for this pedigree (LOD = 2.3 at $q = 0$ cM).

Microarray data from the genome-wide linkage study of Pedigree 441 were further analyzed for CNVs, using the Copy Number Analyser for GeneChip® (CNAG) Ver. 2.0 (32) and PennCNV(33) software packages. A large duplication was identified within the linked interval on chromosome 12q14 that spans ~690 kbp and extends from 62 980 to 63 670 kbp (Fig. 2). This duplication was detected in all 10 affected family members, using the same CNV analysis and was absent from the Database of Genomic Variants (34). The presence of this chromosome 12q14 duplication was confirmed with three separate comparative genomic hybridization (CGH) experiments. DNA from one family member with NTG (Fig. 1A, Subject II-4) was analyzed using CGH microarrays with (i) 385 000 probes distributed across the genome, (ii) 2 100 000 probes distributed across the genome, and finally (iii) 72 000 probes distributed across the chromosome 12q14 locus with a mean probe spacing of 151 bps (NimbleGen, Madison, WI, USA). All three CGH experiments confirmed the presence and the location of a large duplication on chromosome 12q14. The hybridization data produced by the commercially available genome-wide CGH microarrays reported a duplication extending from 63 020 to 63 680 kbp on chromosome 12q14 (Fig. 2), whereas the custom chromosome 12q14 CGH array identified slightly different borders of the same duplication that spans from 62 900 to 63 680 kbp (Fig. 2). To further validate the duplication detected by the SNP analysis and the CGH experiments, we developed a quantitative polymerase chain reaction (qPCR) assay that is specific for TANK-binding kinase 1 (*TBK1*), one of the genes within the chromosome 12q14 duplication. Amplification of *TBK1* from the DNA samples of all affected family members of Pedigree 441 reached PCR threshold levels at an average of 0.5 cycles earlier than control subjects, which is consistent with the existence of an extra copy of the *TBK1* gene and additionally confirms the presence of the chromosome 12q14 duplication (data not shown). Three different methods (SNP analysis, CGH and qPCR) all show that members of Pedigree 441 with NTG have a large duplication on chromosome 12q14.

Linkage analysis and CNV studies of Pedigree 441 suggest that a chromosome 12q14 duplication that spans four genes (*TBK1*, *XPOT*, *RASSF3* and *GNS*) is responsible for the NTG that runs in the family (Fig. 2). Each of the genes contained within the duplication was evaluated as a candidate for causing glaucoma with gene expression studies. As NTG

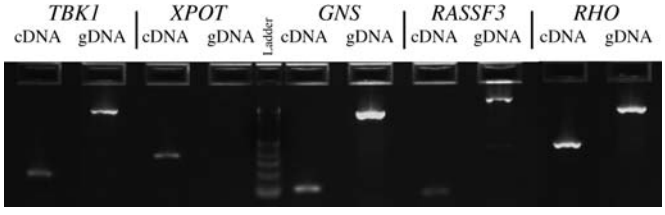

Figure 3. *TBK1* expression in the human retina. RNA from human retina was used as a template in RT-PCR assays designed for genes encompassed by the chromosome 12q14 duplication in Pedigree 441 (*TBK1*, *XPOT*, *RASSF3*, *GNS*) and the control gene rhodopsin (*RHO*). Each assay used primers located entirely within neighboring exons and spanned an intron. Production of appropriate-sized amplicons demonstrated that each gene is expressed in the human retina. Control lanes with genomic DNA produced larger amplicons due to the included intron sequence.

is a disease that primarily affects the optic nerve and ganglion cells of the neurosensory retina, we investigated the expression of the duplicated chromosome 12q14 genes in the human retina with reverse-transcription (RT)-PCR. Amplification of the four genes from retinal cDNA showed that they are all expressed in this tissue (Fig. 3) and thus are plausible candidates for causing NTG.

The effect of the chromosome 12q14 duplication on the expression level of the four encompassed genes (*TBK1*, *XPOT*, *RASSF3* and *GNS*) was assessed with microarrays. First, skin fibroblasts were obtained from three members of family 441 with the duplication (Fig. 1A: II-3, II-4, II-5) and three control subjects. Gene expression was assessed by analyzing RNA isolated from fibroblast cells with Affymetrix GeneChip Exon 1.0 ST microarrays. After normalization using the robust multi-array average (RMA) metric, 38 annotated genes were found to have a >1.5-fold difference in expression in patients when compared with controls with a P-value <0.05 (Supplementary Material, Table S1). When this experiment was repeated with three additional family members with the duplication (Fig. 1A: III-1, III-6, III-7) and three additional controls, 31 annotated genes were found to have a >1.5-fold difference in expression in patients when compared with controls with a P-value <0.05 (Supplementary Material, Table S1). Only one gene, *TBK1*, was identified as having consistently altered expression levels in the presence of the chromosome 12 duplication in both of these independent experiments. Expression of *TBK1* was found to be elevated 1.60-fold when expression array data from both experiments were pooled ($P = 0.00074$, Table 2). When other genes located within the chromosome 12 duplication (*XPOT*, *RASSF3* and *GNS*) were specifically examined using the pooled data, the expression of *GNS* was found to be $\sim$1.5-fold greater in patients than in controls, but had a P-value >0.05 in one of the individual experiments (Table 2). Only minimal differences in expression of *XPOT* and *RASSF3* were detected between patients and controls (Table 2). This experiment showed that the chromosome 12q14 duplication in Pedigree 441 is associated with increased transcription of *TBK1* as well as *GNS*.

The role of chromosome 12q14 duplication in individual cases of glaucoma was assessed by testing a cohort of 400 glaucoma patients, 74 of which have NTG, 100 normal control subjects and 400 age-related macular degeneration (AMD) patients. These glaucoma patients, normal control subjects and AMD patients had been genotyped at over 500 000 SNPs as part of a previous genome-wide association study (GWAS) (data not shown). CNV analyses of these SNPs showed that two of the 74 NTG patients (Subject 458-1 and Subject 1159-1) each had unique chromosome 12q14 duplications that overlapped the duplication detected in Pedigree 441 (Fig. 2). The duplications in patients 458-1 and 1159-1 were confirmed with a custom chromosome 12 CGH array (data not shown). The smallest duplication (300 kbp) was detected in patient 1159-1, who had a maximum IOP of 20 mmHg and no family history of glaucoma. A 650 kbp duplication was detected in patient 458-1 (Fig. 2). Patient 458-1 had a strong family history of POAG with low or borderline IOP (Subject IV-1 in Fig. 1B), and clinical features of the glaucoma in his family are shown in Table 1 and have been previously described (35). DNA was available from three additional members of this family with NTG and three family members with unknown glaucoma status. All of the members of Pedigree 458 with glaucoma were found to have a chromosome 12q14 duplication, using the qPCR assay described above, although none of the members with unknown glaucoma status had the duplication. No duplications in this region were detected in any of the 326 glaucoma patients with elevated IOP, nor were they detected in 100 normal control subjects, 400 AMD patients, or in the Database of Genomic Variants (34). Finally, an additional 78 more NTG patients were subsequently tested for CNVs, using the qPCR assay described above, and no additional chromosome 12q14 duplications were detected. These data suggest that duplication of chromosome 12q14 not only leads to NTG in Pedigree 441, but also may have a role in $\sim$1.3% (2 of 152) of cases of NTG. Furthermore, the smallest duplication (300 kbp) was detected in NTG patient 1159-1 and encompassed *TBK1*, *XPOT* and portions of *RASSF3* (Fig. 2), thus narrowing the number of completely duplicated genes to *TBK1* and *XPOT*.

Of the four genes encompassed by the duplication detected in Pedigree 441, additional study was focused on *TBK1* as the prime candidate for causing glaucoma because it was the only gene that showed significant differential gene expression in our microarray studies (Table 2) and was included within all three detected duplications (Fig. 2). Consequently, *TBK1* expression was further assessed with northern blot analysis (Fig. 4). RNA from fibroblast cells was collected from NTG patients with the chromosome 12q14 duplication ($n = 7$) and from control subjects without the duplication ($n = 5$). Northern blot analysis of these RNA samples with a *TBK1* probe produced a single band at the expected size for a single *TBK1* transcript (3.0 kbp). *TBK1* expression in the northern blot was quantified using densitometry and was normalized to the expression of β-actin. Expression of *TBK1* in patients with the chromosome 12q14 duplication was found to be 1.48-fold greater than in controls without the duplication ($P = 0.015$). This experiment confirmed that the duplication of the *TBK1* gene has a significant effect on its transcription and was in close agreement with the expression data from the microarray experiments.

The localization of TBK1 protein was next evaluated within the retina by performing immunohistochemistry, using a

Table 2. Comparison of gene expression between patients with the chromosome 12 duplication and controls

	Cohort	*P*-value	Fold change	Control mean log 2 signal strength ($n = 3$)	Patient mean log 2 signal strength ($n = 3$)
Genes with consistent differential expression					
TBK1	Cohort 1 ($n = 6$)	0.038	1.55	6.97	7.59
	Cohort 2 ($n = 6$)	0.045	1.61	6.61	7.30
	Combined 1 and 2 ($n = 12$)	0.00074	1.60	6.80	7.47
Genes in the chromosome 12 duplication					
XPOT	Cohort 1 ($n = 6$)	0.11	1.21	9.01	9.28
	Cohort 2 ($n = 6$)	0.12	1.09	8.46	8.59
	Combined 1 and 2 ($n = 12$)	0.047	1.17	8.62	8.85
TBK1	Cohort 1 ($n = 6$)	0.038	1.55	6.97	7.59
	Cohort 2 ($n = 6$)	0.045	1.61	6.61	7.30
	Combined 1 and 2 ($n = 12$)	0.00074	1.60	6.80	7.47
RASSF3	Cohort 1 ($n = 6$)	0.64	1.08	4.55	4.66
	Cohort 2 ($n = 6$)	0.92	−1.01	4.36	4.34
	Combined 1 and 2 ($n = 12$)	0.82	1.02	4.42	4.45
GNS	Cohort 1 ($n = 6$)	0.0062	1.61	7.66	8.35
	Cohort 2 ($n = 6$)	0.055	1.44	7.59	8.12
	Combined 1 and 2 ($n = 12$)	0.00034	1.52	7.67	8.27

Gene expression in NTG patients with the chromosome 12 duplication was compared with controls, using Affymetrix GeneChip Exon 1.0 ST microarrays. In Cohort 1, gene expression was analyzed using RNA from skin fibroblast cells from three family members with the duplication (Fig. 1A: II-3, II-3 and II-5) and from three control subjects. In Cohort 2, three additional family members with the duplication (Fig. 1A: III-1, III-6 and III-7) and three additional control subjects were similarly studied. Genes that were found to have a log2 signal strength <5.0 in any subjects were eliminated from the analysis. Those genes that had a >1.5-fold difference in the expression level in patients when compared with controls with a *P*-value <0.05 in studies of both cohorts of patients are shown in the top section of the table. The expression levels of genes (*XPOT*, *TBK1*, *RASSF3* and *GNS*) that are located within the chromosome 12 duplication were specifically examined and are shown in the bottom section of the table.

monoclonal anti-TBK1 antibody on sagittal sections of human donor eye tissues. In studies of five eyes, TBK1 antibodies labeled ganglion cells, the retinal nerve fiber layer and the microvasculature (Fig. 5A and B), indicating that TBK1 protein is present in tissues affected by glaucoma.

Finally, *TBK1*, was further evaluated as a candidate for causing glaucoma by testing a cohort of 274 glaucoma patients (136 of which had NTG) and 145 controls for disease-causing mutations with a combination of single-strand conformation polymorphism (SSCP) analysis, high-resolution melt (HRM) analysis and DNA sequencing. A total of five DNA sequence variants were identified (Table 3), including three non-synonymous codon variations (Ser151Phe, Leu306Ile and Val464Ala). However, when analyzed individually or as a group, none of the non-synonymous codon variations was detected in patients at a statistically higher frequency than in controls ($P > 0.05$).

DISCUSSION

We have discovered a novel locus for open-angle glaucoma (*GLC1P*) on chromosome 12q14 using linkage analysis of Pedigree 441 (Fig. 1A). A range of techniques (SNP analysis, CGH and qPCR) have shown that a large duplication within the *GLC1P* locus is co-inherited with NTG in Pedigree 441 and is absent from controls and from a database of known CNVs (34). Additional overlapping CNVs were identified in two NTG patients, one of which was co-inherited with glaucoma in a large pedigree (Fig. 1B). To our knowledge, this is the first example of CNVs that are associated with an open-angle glaucoma locus, and their prevalence in our cohort of unrelated NTG subjects (1.3%) suggests that duplication of chromosome 12q14 may be the most common known molecular basis of NTG. Furthermore, the chromosome 12q14 duplication was first discovered with studies of a pedigree with African-American ancestry, which may suggest a more common role of similar CNVs in cohorts of African-American NTG patients. However, two of the three NTG subjects found to carry chromosome 12q14 duplications had strong family histories of NTG, which suggests that extrapolating the frequency of this duplication to sporadic cases of NTG should be done with caution. Furthermore, data to assess the penetrance of this CNV are limited at present to the two relatively small families we have identified (Pedigrees 441 and 458).

It is interesting to note that the *GLC1P* locus coincides with the genetic locus for another optic nerve disease, cavitary optic disc anomalies (CODA) that we have previously mapped to chromosome 12q (36). There are some clinical similarities between CODA and NTG. Patients with CODA have optic discs that are congenitally excavated and may become progressively cupped in the absence of elevated IOP (37). Given the clinical similarities and the overlapping genetic loci, it is tempting to hypothesize that some cases of NTG and CODA are allelic conditions and may be the result of defects in the same gene, i.e. one of the genes that are duplicated in Pedigree 441. However, we have tested our large pedigree with CODA for CNVs that overlap those detected in our NTG subjects, and no duplications or deletions were identified with qPCR and Nimblegen CGH arrays (data not shown).

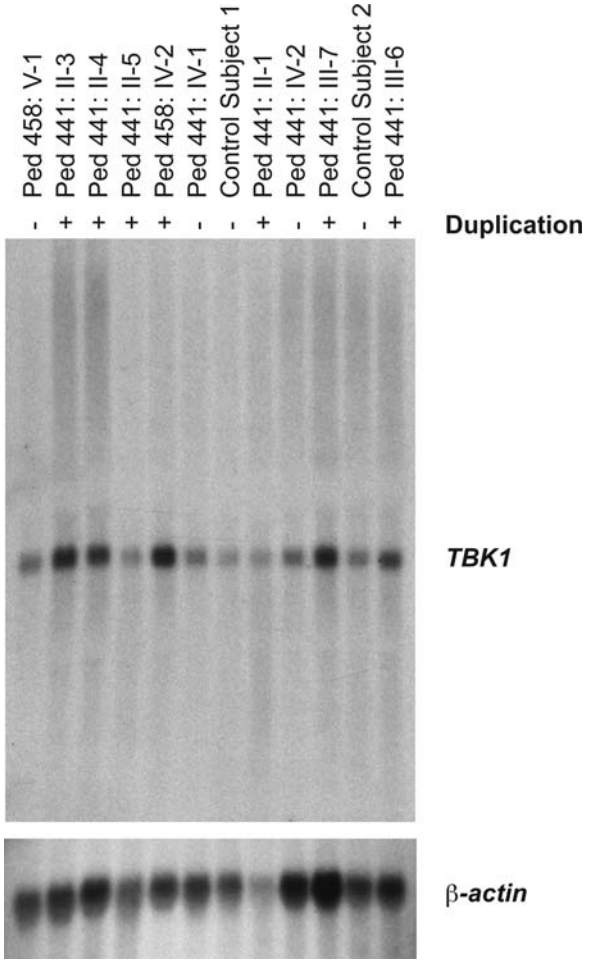

Figure 4. Northern blot analysis of *TBK1*. Expression of *TBK1* in patients with the chromosome 12q14 duplication ($n = 7$) was compared with expression in subjects without the duplication ($n = 5$) by northern blot analysis of RNA collected from fibroblast cells cultured from skin biopsies. Total RNA from fibroblast cells was first probed with a *TBK1* cDNA probe. The blot was then stripped and re-probed with a β-actin (*ACTB*) clone. Probing with the *TBK1* clone produced a single band that was quantified using the IMAGE software package and normalized to expression level of *ACTB*. When compared with control subjects, expression of *TBK1* in patients with the chromosome 12q14 duplication was elevated 1.48-fold ($P = 0.015$).

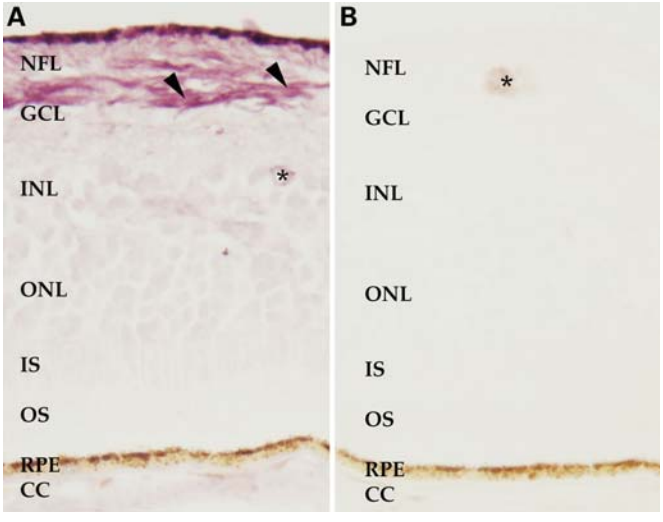

Figure 5. Immunohistochemistry. (**A**) Representative immunohistochemical labeling of TBK1 in human donor retina shows localization to the retinal ganglion cells and axon bundles (arrows), as well as to the retinal microvasculature (asterisks). (**B**) No primary antibody negative control. The layers of the retina are indicated by abbreviations: NFL, nerve fiber layer; GCL, ganglion cell layer; INL, inner nuclear layer; ONL, outer nuclear layer; IS, inner segments; OS, outer segments; RPE, retinal pigment epithelium; CC, choriocapillaris. Some minor peroxidase reactivity is present within intravascular erythrocytes in the 'no-primary antibody' control panel.

Although the precise mechanism by which duplication of chromosome 12q14 leads to NTG in our patients is unknown, it likely involves dysregulation of gene expression. It is plausible that an extra copy of the encompassed genes leads to a pathologic increase in expression. Such gene dosage mechanisms of disease are well described, as with the duplication of the *PMP22* gene in Charcot–Marie–Tooth disease (38–41) and with the duplication of beta-amyloid gene in Alzheimer disease (42). Alternatively, it is possible that the chromosomal re-arrangements in our patients not only result in a duplication of several genes, but also reposition enhancer elements that alter expression of genes neighboring the re-arrangement borders. This mechanism of disease is known to cause some cases of Axenfeld–Rieger syndrome (29). Chromosomal re-arrangements can also cause alterations in the tissue specificity of gene expression (43) or can cause disease by directly disrupting genes.

Linkage analysis of Pedigree 441 produced an LOD score of 2.7 at chromosome 12q14, which suggests this region of the genome contains the family's NTG gene, although this LOD score is slightly below the threshold of 3.0 for statistical significance. A subsequent search for CNVs in the family identified a duplication within the chromosome 12q14 locus that spans four genes, *XPOT*, *TBK1*, *RASSF3* and *GNS*. The four duplicated genes became our top candidates; however, as with all linkage-based studies, it remained possible that other genes in the linked region have a role in this family's glaucoma. To identify which of these four genes is likely responsible for NTG in Pedigree 441, we conducted a series of additional experiments. Although RT-PCR experiments showed that all four genes are transcribed in the human retina (Fig. 3), the duplication led to altered expression in only two of these genes, *TBK1* and *GNS* (Table 2). Given these expression data, *TBK1* and *GNS* became the top candidates for causing NTG in out patients. Subsequent discovery of a smaller chromosome 12q14 duplication in a single NTG patient (patient 1159-1, Fig. 2) that spanned *TBK1* but not *GNS* provided some support for *TBK1* as the glaucoma-causing gene in the region. However, it does remain possible that chromosome 12q14 duplications lead to glaucoma by their effects on the expression of genes that are nearby but not always duplicated themselves, such as *GNS*. Immunohistochemical studies showed that TBK1 is expressed in the ganglion cells and in the microvascular of the human retina (Fig. 5). Accordingly, *TBK1* is active in the correct ocular tissues to have a role in proposed apoptotic or vascular mechanisms of disease in glaucoma. Overall, these studies and

Table 3. Mutation screening data

Variation	NTG	POAG	Control	*P*-value		
	$n = 136$	$n = 138$	$n = 145$	NTG versus controls	POAG versus controls	Glaucoma versus controls
Synonymous changes						
Asn22Asn	15	14	24	0.23	0.12	0.090
Ile326Ile	0	2	0	>0.99	0.24	0.55
Total	15	16	24	0.23	0.24	0.17
Non-synonymous changes						
Ser151Phe	0	1	0	>0.99	0.49	>0.99
Leu306Ile	2	0	0	0.23	>0.99	0.55
Val464Ala	4	10	5	>0.99	0.19	0.62
Total	6	11	5	0.76	0.12	0.26

NTG subjects ($n = 136$), POAG subjects ($n = 138$) and control subjects ($n = 145$) were tested for disease-causing mutations in the coding sequence of *TBK1*, using a combination of SSCP analysis, HRM analysis and DNA sequencing. None of the non-synonymous coding sequence variants are statistically associated with NTG or POAG when analyzed alone or as a group ($P > 0.05$). The *P*-values presented have not been corrected for multiple measures.

observations suggest that the chromosome 12q14 duplication may lead to NTG via a dysregulation of *TBK1* expression.

In addition to searching for CNVs that affected *TBK1*, we also searched for coding sequence variations that might be associated with glaucoma. Three rare variants (Ser151Phe, Leu306Ile and Val464Ala) were detected in glaucoma patients. Although we were unable to show that any of these variants are associated with glaucoma individually or as a group, the sample size of the cohort is small ($n = 274$). It remains possible that a larger study or functional studies may be able to show that one or more of these rare *TBK1* coding sequence variants are involved in glaucoma pathogenesis. Furthermore, when we examined data from our prior GWAS, no evidence of an as-yet-undiscovered ancestral risk factor for glaucoma was detected at the *TBK1* locus (data not shown).

TBK1 is a kinase that regulates the activation of genes in the NF-κB pathway (44) and is an excellent candidate for causing NTG. Several lines of evidence link *TBK1* with NTG. First, we have shown that *TBK1* is expressed in key tissues involved in glaucoma pathophysiology, the ganglion cells and the nerve fiber layer of the human retina (Figs 3 and 5). Second, *TBK1* is known to interact with *OPTN*, the only previously described NTG gene (11). Yeast two-hybrid studies have shown that TBK1 protein binds to OPTN. Furthermore, interaction between these proteins is greatly enhanced by a glaucoma-associated mutation (E50K) in *OPTN* (45). These connections with a known NTG gene and an NTG-causing mutation further implicate *TBK1* in glaucoma pathogenesis. Finally, it is biologically plausible that dysregulation of *TBK1* expression might lead to glaucoma. *TBK1* encodes a serine/threonine kinase that regulates the expression of genes in the NF-κB pathways. This signaling pathway regulates important processes that have been implicated in the pathogenesis of glaucoma, including apoptosis and modulation of the immune system. Together, these data strongly suggest that duplication of chromosome 12q14 and *TBK1* may lead to NTG and also provide additional support for a role of NF-κB pathways in glaucoma pathogenesis as first suggested by studies of optineurin (11). However, the most definitive evidence may require the development of transgenic animal models that recapitulate this glaucoma phenotype.

MATERIALS AND METHODS

Glaucoma subjects and controls

The study was approved by the University of Iowa's Institutional Review Board and informed consent was obtained from study participants. Patients were examined by fellowship-trained glaucoma specialists and received complete ophthalmic examinations (including gonioscopy, standardized visual field testing and stereoscopic optic nerve examination) and were diagnosed with open-angle glaucoma when characteristic optic nerve damage and corresponding visual field defects were detected in at least one eye as previously described (46). NTG was diagnosed when the maximum IOP was ≤21 mmHg in both eyes. This IOP threshold for diagnosing NTG was used without adjustment for central corneal thickness (CCT). Some subjects may have had a maximum IOP of >21 if their IOP were adjusted for CCT. However, as there is no consensus for an algorithm to make such a correction, we opted to use uncorrected IOPs in our study. Four categories of subjects were enrolled in the study: (i) *Glaucoma pedigrees*. Twelve family members of an African-American pedigree (Pedigree 441, Fig. 1A) from Maryland were enrolled as study subjects and 10 were diagnosed with POAG. Some members of this pedigree had been followed for over 20 years and all but one of the subjects with glaucoma also met criteria for a diagnosis of NTG, and one family member had POAG with a maximum IOP of 22 mmHg. Similarly seven members of a Caucasian NTG pedigree from Iowa (Pedigree 458, Fig. 1B) were enrolled as study subjects. Clinical features of members of this pedigree have been previously described (35). (ii) *Glaucoma cohort*. Four hundred unrelated open-angle glaucoma patients from Iowa (74 of which had NTG) were enrolled as study subjects and were part of a prior GWAS. Additional POAG and NTG patients from Iowa were enrolled for follow-up studies as described in Quantitative RT-PCR analyses and Mutation screening of *TBK1* sections. Thirty-eight (51%) of the 74 NTG subjects have a self-reported family history of glaucoma. (iii) *Normal control cohort*. One hundred unrelated subjects over 50 years of age from Iowa that had no evidence of glaucomatous optic nerve damage with stereoscopic ophthalmoscopy and had an IOP of ≤21 mmHg were enrolled as control subjects. These

subjects were also part of a prior GWAS. (iv) *AMD cohort*. Four hundred unrelated subjects with macular degeneration from Iowa that were part of a prior GWAS were also enrolled for this study. These AMD subjects had no history of glaucoma and a maximum IOP of $\leq$21 mmHg and were judged to have normal optic discs by board-certified ophthalmologists. Blood samples were obtained from study participants and DNA was prepared using a non-organic method (47). Two members of Pedigree 441 (Fig. 1, II-5 and III-3) were tested for mutations in previously reported glaucoma genes (myocilin OMIM 601652; optineurin OMIM 602432), using previously described assays (12,14), and no mutations were detected (data not shown).

Linkage analysis

Members of Pedigree 441 were genotyped with STRP genetic markers flanking myocilin and optineurin, and linkage to these genes was ruled out using standard methods as previously described (48). A genome-wide scan was next performed on all 10 family members with NTG, using Illumina660W-Quad microarrays (Illumina, San Diego, CA, USA), which interrogate 660 000 SNPs. Sample processing and labeling were performed using the manufacturer's instructions at GeneSeek (Lincoln, NE, USA). Multipoint NPL scores were calculated from genotypes of Pedigree 441, using the MERLIN software package (49). Pairwise linkage analysis using STRP markers was performed with the MLINK and LODSCORE programs as implemented in the FASTLINK (v2.3) version (50,51) of the LINKAGE software package (52). Penetrance and disease gene frequency were set to 99 and 0.001%, respectively. For each STRP marker, the allele frequencies were assumed to be equal. True allele frequencies could not be reliably estimated from the small number of spouses available in the pedigree. In order to show that the assumption of the equal allele frequencies would not significantly affect our linkage results, we recalculated the LOD scores using allele frequencies for the 'affected' allele of the most tightly linked marker (D12S359) ranging from 0.01 to 0.5. The Zmax for D12S359 was 2.3 when the 'affected' allele frequency was arbitrarily set to 50%. This shows that our assumption of equal allele frequencies was reasonable and does not significantly affect the results of our calculations.

CNV analysis

Family members of Pedigree 441 were also typed with Affymetrix microarrays (*Nsp1* array of the GeneChip Human Mapping 500K Array Set, Affymetrix, Santa Clara, CA, USA) which interrogate 262 000 SNPs for CNV analysis. Sample processing and labeling were performed using the manufacturer's instructions. To detect changes in copy number, we used a publicly available program, CNAG Ver. 2.0 (32). Statistically significant deviations in signal intensity between SNPs on the test and reference arrays are detected using a hidden Markov model (HMM). Five to 10 'best fit' reference arrays drawn from a set of over 1000 *Nsp*I and *Sty*I Affymetrix arrays are loaded in its local memory. To identify these 'best fit' reference arrays, the signal intensity standard deviation values are ranked according to their similarity to each new test array. The arrays with the highest ranked standard deviation values are used as the reference set for each new test array. Each test array was referenced to at least six other arrays of unrelated individuals with similar signal intensity standard deviations. CNAG then applied an HMM to the data and provided a graphical output by chromosome. The HMM highlighted chromosomal regions with significant deviation in signal intensity and CNVs were then manually detected and annotated. Arrays with high log *R* ratio standard deviations resulting in fewer than six appropriate references were not included in the final analysis. Arrays with more than 30 CNVs were removed from the final results as part of the array-based quality control. CNVs called by fewer than five SNPs or $<$1 kb were also removed from the final results.

Array-based CGH experiments

One microgram of patient DNA and 1 μg of reference DNA (Promega) were fluorescently labeled in parallel, followed by co-hybridization to a Nimblegen 385 K array, a 2.1 M array or a custom chromosome 12q14 array. Arrays were scanned using a GenePix 4000B, and signal intensity data were analyzed using the segMNT algorithm within the NimbleScan software. The SignalMap software was used to visualize the array CGH data as a graphical output.

Quantitative RT-PCR analyses

All quantitative RT-PCR analyses were performed in triplicate for each DNA sample. Two amplicons were amplified. One amplicon was within a gene (*TBK1*) in the duplication detected by array studies on chromosome 12q14 and another amplicon was within a control gene (*RHO*) on a different chromosome. The qPCR analyses were performed according to the manufacturer's protocol with standard conditions (Bio-Rad, Hercules, CA, USA). The threshold cycle value was calculated using the delta C_T method. C_T was determined using the thermocycler software and an average of the three replicates was calculated. Average C_T values of the triplicate reaction for *TBK1* amplicon were compared with average C_T values for the control gene, *RHO* to normalize for amplicon amplification efficiency and for small variations in the quantity of DNA template. Results from each affected family member of Pedigree 441 were separately compared with four different control samples. The same qPCR analysis was also performed on DNA samples from an additional cohort of 78 NTG patients and 78 ethnically matched controls from Iowa.

RNA isolation

RNA was isolated from skin fibroblast cells at the fourth passage with the RNeasy Kit (Qiagen, Valencia, CA, USA), using the manufacturer's stand protocol. RNA was treated with DNAse I, purified with ethanol precipitation, quantified with the Quant-iT RiboGreen RNA Assay Kit (Molecular Probes, Eugene, OR, USA) and assayed for integrity on a model 210 bioanalyzer (Agilent Technologies, Inc., Palo Alto, CA, USA).

Microarray expression analysis

Gene expression studies were performed on RNA from fibroblast cells cultured from skin biopsies in a two-step experiment comparing expression between NTG patients with the chromosome 12q14 duplication and control subjects without the duplication. The first experiment included three NTG patients in Pedigree 441 with the duplication (Fig. 1: II-3, II-4 and II-5) and three control subjects without the duplication (Fig. 1A: Pedigree 441, IV-1 and IV-2, and from an unrelated control subject). The second experiment included three different NTG patients in Pedigree 441 with the duplication (Fig. 1: III-1, III-6, III-7) and three unrelated controls without the duplication. The NTG patients from Pedigree 441 used in this analysis were all African American (five females and one male) with an average of 50 years of age at the time of skin biopsy. The control subjects for this analysis had no history of glaucoma and included three females and three males with an average of 31 years of age at the time of skin biopsy. Of the six control subjects, two were of African-American ancestry (members of Pedigree 441, Subjects IV-1 and IV-2), three were Caucasian (including control Subject V-1 in Pedigree 458) and ethnicity data were unavailable for an additional control subject. RNA was converted to Affymetrix compatible cRNA following the manufacturer's standard protocols and hybridized to Affymetrix GeneChip Exon 1.0 ST microarrays. Raw data were normalized using the RMA algorithm and analyzed using the Partec Genomics Suite 6.5 software package. Probe sets that produced a normalized log 2 signal strength of less than 5.0 for any sample were eliminated from the analysis. A threshold of >1.5-fold change in expression level using a base-2 log scale with a P-value of <0.05 was used to identify genes with differential expression between patients and controls. A subset of genes that were differentially expressed between patients and controls in both of the independent experiments were identified using these criteria. Finally, data from both experiments were pooled and a similar comparison of patients ($n = 6$) versus controls ($n = 6$) was conducted.

Northern blot analysis

Fibroblast RNA from seven subjects affected with NTG and carriers of the chromosome 12q14 duplication and from five controls was electrophoresed, electroblotted and probed with a ^{32}P radio-labeled full-length *TBK1* cDNA clone (Origene, Rockville, MD, USA) by Lofstrand Labs Limited (Gaithersburg, MD, USA) using standard techniques. The blot was stripped and reprobed with the control gene β-actin. Blots were exposed to film at -70°C for 24 h and the bands produced from the *TBK1* probe were quantified using the public domain NIH Image program (available at http://rsb.info.nih.gov/nih-image/) and were normalized to bands produced by the β-actin probe. The mean expression of *TBK1* RNA in fibroblasts from patients with a *TBK1* duplication was compared with that of controls without a duplication, using a *t*-test.

Immunohistochemistry

Human donor eyes were obtained from the Iowa Lions Eye Bank and were processed by fixation in 4% paraformaldehyde within 8 h of death. Cryostat sections of posterior poles spanning from the macula to the ora serrata containing both retina and retinal pigment epithelium/choroid were collected. Sections were blocked in 1% horse serum for 15 min. The anti-TBK1 primary antibody was raised in a mouse and was used at a concentration of 1 μg/ml (Calbiochem, Gibbstown, NJ, USA). Immunolabeling was performed as described previously (35).

Mutation screening of *TBK1*

A cohort of 274 POAG patients (136 of which had NTG) and 145 control subjects from Iowa were tested for disease-causing mutations in *TBK1*, using either SSCP analysis or HRM analysis. Of the 136 NTG patients tested for *TBK1* coding sequence mutations, 58 were among the 400 glaucoma patients who were tested for CNVs by re-analyzing SNP data that were available from a prior GWAS. For SSCP analysis, 12.5 ng of each patient's DNA were used as a template in a 8.35 μl of PCR solution containing: 1.25 μl of 10× buffer (100 mM Tris–HCL, pH 8.3, 500 mM KCl, 15 mM MgCl2), 300 μm of each dCTP, dATP, dGTP and dTTP, 1 pmol of each primer and 0.25 U Biolase polymerase (Biolase). The oligonucleotide primer sequences are available on request. Samples were denatured for 5 min at 94°C and incubated for 35 cycles under the following conditions: 94°C for 30 s, 55°C for 30 s, 72°C for 30 s in a DNA thermocycler (Bio-Rad). After amplification, 5 μl of stop solution (95% formamide, 10 mM NaOH, 0.05% bromophenol blue, 0.05% xylene cyanol) was added to each sample. Amplification products were denatured for 3 min at 94°C and electrophoresed on 6% polyacrylamide and 5% glycerol gels at 25 W for ∼3 h at room temperature. Following electrophoresis, gels were stained with silver (53). Abnormal PCR products identified by SSCP analysis were bi-directionally sequenced using fluorescent dideoxynucleotides on an Applied Biosystems (ABI) model 3730 automated sequencer. For HRM, 12.5 ng of each patient's DNA were used as a template in a 10 μl PCR solution containing 5 μl of SsoFast EvaGreen Supermix (Bio-Rad) and 1 pmol of each primer. The thermocycling profile was carried out on a Bio-Rad CFX96 Real-Time System using the following profile: denature at 95°C for 2 min, followed by 40 cycles of 95°C for 10 s, 55°C for 10 s and 72°C for 15 s. The amplified DNA then underwent HRM mapping under the following conditions: 95°C for 10 s, followed by an incremental temperature increase of 0.5°C with a hold of 5 s per increment. The melt curves generated were analyzed using Precision Melt Analysis™ Software v1.0 (Bio-Rad). Amplified DNA with abnormal HRM profiles were identified and then bi-directionally sequenced using fluorescent dideoxynucleotides on an ABI model 3730 automated sequencer. The frequency of non-synonymous *TBK1* mutations was compared between patients and controls individually and as a group using Fisher's exact test and the software package R.

SUPPLEMENTARY MATERIAL

Supplementary Material is available at *HMG* online.

ACKNOWLEDGEMENTS

We would also like to acknowledge our research project coordinator, Mari Long, for her invaluable contributions.

Conflict of Interest statement. None declared.

FUNDING

This work was supported by Research to Prevent Blindness, the Gustavus and Louise Pfeiffer Research Foundation, the Marlene S. and Leonard A. Hadley Glaucoma Research Fund and the National Institutes of Health (RO1EY018825 and K08 EY017698 to J.H.F. and R01EY010564 to V.C.S.).

REFERENCES

1. Tielsch, J.M., Katz, J., Singh, K., Quigley, H.A., Gottsch, J.D., Javitt, J. and Sommer, A. (1991) A population-based evaluation of glaucoma screening: the Baltimore Eye Survey. *Am. J. Epidemiol.*, **134**, 1102–1110.
2. Congdon, N., O'Colmain, B., Klaver, C.C., Klein, R., Munoz, B., Friedman, D.S., Kempen, J., Taylor, H.R. and Mitchell, P. (2004) Causes and prevalence of visual impairment among adults in the United States. *Arch. Ophthalmol.*, **122**, 477–485.
3. Resnikoff, S., Pascolini, D., Etya'ale, D., Kocur, I., Pararajasegaram, R., Pokharel, G.P. and Mariotti, S.P. (2004) Global data on visual impairment in the year 2002. *Bull. World Health Organ.*, **82**, 844–851.
4. Quigley, H.A. and Broman, A.T. (2006) The number of people with glaucoma worldwide in 2010 and 2020. *Br. J. Ophthalmol.*, **90**, 262–267.
5. Friedman, D.S., Wolfs, R.C., O'Colmain, B.J., Klein, B.E., Taylor, H.R., West, S., Leske, M.C., Mitchell, P., Congdon, N. and Kempen, J. (2004) Prevalence of open-angle glaucoma among adults in the United States. *Arch. Ophthalmol.*, **122**, 532–538.
6. Challa, P. (2008) Glaucoma genetics. *Int. Ophthal. Clin.*, **48**, 73–94.
7. Baird, P.N., Foote, S.J., Mackey, D.A., Craig, J., Speed, T.P. and Bureau, A. (2005) Evidence for a novel glaucoma locus at chromosome 3p21-22. *Hum. Genet.*, **117**, 249–257.
8. Fan, B.J., Ko, W.C., Wang, D.Y., Canlas, O., Ritch, R., Lam, D.S. and Pang, C.P. (2007) Fine mapping of new glaucoma locus GLC1M and exclusion of neuregulin 2 as the causative gene. *Mol. Vis.*, **13**, 779–784.
9. Wang, D.Y., Fan, B.J., Chua, J.K., Tam, P.O., Leung, C.K., Lam, D.S. and Pang, C.P. (2006) A genome-wide scan maps a novel juvenile-onset primary open-angle glaucoma locus to 15q. *Invest. Ophthalmol. Vis. Sci.*, **47**, 5315–5321.
10. Stone, E.M., Fingert, J.H., Alward, W.L., Nguyen, T.D., Polansky, J.R., Sunden, S.L., Nishimura, D., Clark, A.F., Nystuen, A., Nichols, B.E. *et al.* (1997) Identification of a gene that causes primary open angle glaucoma. *Science*, **275**, 668–670.
11. Rezaie, T., Child, A., Hitchings, R., Brice, G., Miller, L., Coca-Prados, M., Heon, E., Krupin, T., Ritch, R., Kreutzer, D. *et al.* (2002) Adult-onset primary open-angle glaucoma caused by mutations in optineurin. *Science*, **295**, 1077–1079.
12. Fingert, J.H., Heon, E., Liebmann, J.M., Yamamoto, T., Craig, J.E., Rait, J., Kawase, K., Hoh, S.T., Buys, Y.M., Dickinson, J. *et al.* (1999) Analysis of myocilin mutations in 1703 glaucoma patients from five different populations. *Hum. Mol. Genet.*, **8**, 899–905.
13. Kwon, Y.H., Fingert, J.H., Kuehn, M.H. and Alward, W.L. (2009) Primary open-angle glaucoma. *N. Engl. J. Med.*, **360**, 1113–1124.
14. Alward, W.L., Kwon, Y.H., Kawase, K., Craig, J.E., Hayreh, S.S., Johnson, A.T., Khanna, C.L., Yamamoto, T., Mackey, D.A., Roos, B.R. *et al.* (2003) Evaluation of optineurin sequence variations in 1,048 patients with open-angle glaucoma. *Am. J. Ophthalmol.*, **136**, 904–910.
15. Sahlender, D.A., Roberts, R.C., Arden, S.D., Spudich, G., Taylor, M.J., Luzio, J.P., Kendrick-Jones, J. and Buss, F. (2005) Optineurin links myosin VI to the Golgi complex and is involved in Golgi organization and exocytosis. *J. Cell Biol.*, **169**, 285–295.
16. Sarfarazi, M. and Rezaie, T. (2003) Optineurin in primary open angle glaucoma. *Ophthalmol. Clin. North Am.*, **16**, 529–541.
17. Monemi, S., Spaeth, G., Dasilva, A., Popinchalk, S., Ilitchev, E., Liebmann, J., Ritch, R., Heon, E., Crick, R.P., Child, A. *et al.* (2005) Identification of a novel adult-onset primary open-angle glaucoma (POAG) gene on 5q22.1. *Hum. Mol. Genet.*, **14**, 725–733.
18. Hewitt, A.W., Dimasi, D.P., Mackey, D.A. and Craig, J.E. (2006) A Glaucoma Case-control Study of the WDR36 Gene D658G sequence variant. *Am. J. Ophthalmol.*, **142**, 324–325.
19. Fingert, J.H., Alward, W.L., Kwon, Y.H., Shankar, S.P., Andorf, J.L., Mackey, D.A., Sheffield, V.C. and Stone, E.M. (2007) No association between variations in the WDR36 gene and primary open-angle glaucoma. *Arch. Ophthalmol.*, **125**, 434–436.
20. Hauser, M.A., Allingham, R.R., Linkroum, K., Wang, J., LaRocque-Abramson, K., Figueiredo, D., Santiago-Turla, C., del Bono, E.A., Haines, J.L., Pericak-Vance, M.A. *et al.* (2006) Distribution of WDR36 DNA sequence variants in patients with primary open-angle glaucoma. *Invest. Ophthalmol. Vis. Sci.*, **47**, 2542–2546.
21. Pasutto, F., Matsumoto, T., Mardin, C.Y., Sticht, H., Brandstatter, J.H., Michels-Rautenstrauss, K., Weisschuh, N., Gramer, E., Ramdas, W.D., van Koolwijk, L.M. *et al.* (2009) Heterozygous NTF4 mutations impairing neurotrophin-4 signaling in patients with primary open-angle glaucoma. *Am. J. Hum. Genet.*, **85**, 447–456.
22. Vithana, E.N., Nongpiur, M.E., Venkataraman, D., Chan, S.H., Mavinahalli, J. and Aung, T. (2010) Identification of a novel mutation in the NTF4 gene that causes primary open-angle glaucoma in a Chinese population. *Mol. Vis.*, **16**, 1640–1645.
23. Rao, K.N., Kaur, I., Parikh, R.S., Mandal, A.K., Chandrasekhar, G., Thomas, R. and Chakrabarti, S. (2010) Variations in NTF4, VAV2, and VAV3 genes are not involved with primary open-angle and primary angle-closure glaucomas in an Indian population. *Invest. Ophthalmol. Vis. Sci.*, **51**, 4937–4941.
24. Liu, Y., Liu, W., Crooks, K., Schmidt, S., Allingham, R.R. and Hauser, M.A. (2010) No evidence of association of heterozygous NTF4 mutations in patients with primary open-angle glaucoma. *Am. J. Hum. Genet.*, **86**, 498–499; Author reply, 500.
25. Thorleifsson, G., Walters, G.B., Hewitt, A.W., Masson, G., Helgason, A., DeWan, A., Sigurdsson, A., Jonasdottir, A., Gudjonsson, S.A., Magnusson, K.P. *et al.* (2010) Common variants near CAV1 and CAV2 are associated with primary open-angle glaucoma. *Nat. Genet.*, **42**, 906–909.
26. Meguro, A., Inoko, H., Ota, M., Mizuki, N. and Bahram, S. (2010) Genome-wide association study of normal tension glaucoma: common variants in SRBD1 and ELOVL5 contribute to disease susceptibility. *Ophthalmology*, **117**, 1331.e5–1338.e5.
27. Stoilov, I., Akarsu, A.N. and Sarfarazi, M. (1997) Identification of three different truncating mutations in cytochrome P4501B1 (CYP1B1) as the principal cause of primary congenital glaucoma (Buphthalmos) in families linked to the GLC3A locus on chromosome 2p21. *Hum. Mol. Genet.*, **6**, 641–647.
28. Semina, E.V., Retiter, R., Leysens, N.J., Alward, W.L.M., Small, K.W., Datson, N.A., Siegel-Bartelt, J., Bierke-Nelson, D., Bitoun, P., Zabel, B.U. *et al.* (1996) Cloning and characterization of a novel bicoid-related homobox transcription factor gene, RIEG, involved in Reiger Syndrome. *Nat. Genet.*, **14**, 392–399.
29. Nishimura, D.Y., Swiderski, R.E., Alward, W.L., Searby, C.C., Patil, S.R., Bennet, S.R., Kanis, A.B., Gastier, J.M., Stone, E.M. and Sheffield, V.C. (1998) The forkhead transcription factor gene FKHL7 is responsible for glaucoma phenotypes which map to 6p25. *Nat. Genet.*, **19**, 140–147.
30. Nishimura, D.Y., Searby, C.C., Alward, W.L., Walton, D., Craig, J.E., Mackey, D.A., Kawase, K., Kanis, A.B., Patil, S.R., Stone, E.M. *et al.* (2001) A spectrum of FOXC1 mutations suggests gene dosage as a mechanism for developmental defects of the anterior chamber of the eye. *Am. J. Hum. Genet.*, **68**, 364–372.
31. Lines, M.A., Kozlowski, K., Kulak, S.C., Allingham, R.R., Heon, E., Ritch, R., Levin, A.V., Shields, M.B., Damji, K.F., Newlin, A. *et al.* (2004) Characterization and prevalence of PITX2 microdeletions and mutations in Axenfeld–Rieger malformations. *Invest. Ophthalmol. Vis. Sci.*, **45**, 828–833.
32. Nannya, Y., Sanada, M., Nakazaki, K., Hosoya, N., Wang, L., Hangaishi, A., Kurokawa, M., Chiba, S., Bailey, D.K., Kennedy, G.C. *et al.* (2005) A

robust algorithm for copy number detection using high-density oligonucleotide single nucleotide polymorphism genotyping arrays. *Cancer Res.*, **65**, 6071–6079.
33. Wang, K., Li, M., Hadley, D., Liu, R., Glessner, J., Grant, S.F., Hakonarson, H. and Bucan, M. (2007) PennCNV: an integrated hidden Markov model designed for high-resolution copy number variation detection in whole-genome SNP genotyping data. *Genome Res.*, **17**, 1665–1674.
34. Iafrate, A.J., Feuk, L., Rivera, M.N., Listewnik, M.L., Donahoe, P.K., Qi, Y., Scherer, S.W. and Lee, C. (2004) Detection of large-scale variation in the human genome. *Nat. Genet.*, **36**, 949–951.
35. Bennett, S.R., Alward, W.L. and Folberg, R. (1989) An autosomal dominant form of low-tension glaucoma. *Am. J. Ophthalmol.*, **108**, 238–244.
36. Fingert, J.H., Honkanen, R.A., Shankar, S.P., Affatigato, L.M., Ehlinger, M.A., Moore, M.D., Jampol, L.M., Sheffield, V.C., Stone, E.M. and Alward, W.L. (2007) Familial cavitary optic disk anomalies: identification of a novel genetic locus. *Am. J. Ophthalmol.*, **143**, 795–800.
37. Honkanen, R.A., Jampol, L.M., Fingert, J.H., Moore, M.D., Taylor, C.M., Stone, E.M. and Alward, W.L. (2007) Familial cavitary optic disk anomalies: clinical features of a large family with examples of progressive optic nerve head cupping. *Am. J. Ophthalmol.*, **143**, 788–794.
38. Patel, P.I., Roa, B.B., Welcher, A.A., Schoener-Scott, R., Trask, B.J., Pentao, L., Snipes, G.J., Garcia, C.A., Francke, U., Shooter, E.M. *et al.* (1992) The gene for the peripheral myelin protein PMP-22 is a candidate for Charcot–Marie–Tooth disease type 1A. *Nat. Genet.*, **1**, 159–165.
39. Valentijn, L.J., Bolhuis, P.A., Zorn, I., Hoogendijk, J.E., van den Bosch, N., Hensels, G.W., Stanton, V.P. Jr, Housman, D.E., Fischbeck, K.H., Ross, D.A. *et al.* (1992) The peripheral myelin gene PMP-22/GAS-3 is duplicated in Charcot–Marie–Tooth disease type 1A. *Nat. Genet.*, **1**, 166–170.
40. Timmerman, V., Nelis, E., Van Hul, W., Nieuwenhuijsen, B.W., Chen, K.L., Wang, S., Ben Othman, K., Cullen, B., Leach, R.J., Hanemann, C.O. *et al.* (1992) The peripheral myelin protein gene PMP-22 is contained within the Charcot–Marie–Tooth disease type 1A duplication. *Nat. Genet.*, **1**, 171–175.
41. Matsunami, N., Smith, B., Ballard, L., Lensch, M.W., Robertson, M., Albertsen, H., Hanemann, C.O., Muller, H.W., Bird, T.D., White, R. *et al.* (1992) Peripheral myelin protein-22 gene maps in the duplication in chromosome 17p11.2 associated with Charcot–Marie–Tooth 1A. *Nat. Genet.*, **1**, 176–179.
42. Delabar, J.M., Goldgaber, D., Lamour, Y., Nicole, A., Huret, J.L., de Grouchy, J., Brown, P., Gajdusek, D.C. and Sinet, P.M. (1987) Beta amyloid gene duplication in Alzheimer's disease and karyotypically normal Down syndrome. *Science*, **235**, 1390–1392.
43. Miller, M.W., Duhl, D.M., Vrieling, H., Cordes, S.P., Ollmann, M.M., Winkes, B.M. and Barsh, G.S. (1993) Cloning of the mouse agouti gene predicts a secreted protein ubiquitously expressed in mice carrying the lethal yellow mutation. *Genes Dev.*, **7**, 454–467.
44. Pomerantz, J.L. and Baltimore, D. (1999) NF-kappaB activation by a signaling complex containing TRAF2, TANK and TBK1, a novel IKK-related kinase. *EMBO J.*, **18**, 6694–6704.
45. Morton, S., Hesson, L., Peggie, M. and Cohen, P. (2008) Enhanced binding of TBK1 by an optineurin mutant that causes a familial form of primary open angle glaucoma. *FEBS Lett.*, **582**, 997–1002.
46. Alward, W.L., Fingert, J.H., Coote, M.A., Johnson, A.T., Lerner, S.F., Junqua, D., Durcan, F.J., McCartney, P.J., Mackey, D.A., Sheffield, V.C. *et al.* (1998) Clinical features associated with mutations in the chromosome 1 open angle glaucoma gene (*GLC1A*). *N. Engl. J. Med.*, **338**, 1022–1027.
47. Buffone, G.J. and Darlinton, G.J. (1985) Isolation of DNA from biological specimens without extraction with phenol. *Clin. Chem.*, **31**, 164–165.
48. Heon, E., Piguet, B., Munier, F., Sneed, S.R., Morgan, C.M., Forni, S., Pescia, G., Schorderet, D., Taylor, C.M., Streb, L.M. *et al.* (1996) Linkage of autosomal dominant radial drusen (malattia leventinese) to chromosome 2p16-21. *Arch. Ophthalmol.*, **114**, 193–198.
49. Abecasis, G.R., Cherny, S.S., Cookson, W.O. and Cardon, L.R. (2002) Merlin-rapid analysis of dense genetic maps using sparse gene flow trees. *Nat. Genet.*, **30**, 97–101.
50. Cottingham, R.W. Jr, Idury, R.M. and Schaffer, A.A. (1993) Faster sequential genetic linkage computations. *Am. J. Hum. Genet.*, **53**, 252–263.
51. Schaffer, A.A., Gupta, S.K., Shriram, K. and Cottingham, R.W. Jr (1994) Avoiding recomputation in linkage analysis. *Hum. Hered.*, **44**, 225–237.
52. Lathrop, G.M. and Lalouel, J.M. (1984) Easy calculations of lod scores and genetic risks on small computers. *Am. J. Hum. Genet.*, **36**, 460–465.
53. Bassam, B.J., Caetano-Anolles, G. and Gresshoff, P.M. (1991) Fast and sensitive silver staining of DNA in polyacrylamide gels. *Anal. Biochem.*, **196**, 80–83.